

IV.F.1 A Synergistic Approach to the Development of New Hydrogen Storage Materials, Part I

Jeffrey R. Long (Primary Contact),
Jean M.J. Fréchet, Martin Head-Gordon
Dept. of Chemistry
University of California, Berkeley (UCB)
Berkeley, CA 94720-1460
Phone: (510) 642-0860; Fax: (510) 642-8369
E-mail: jrlong@berkeley.edu

Thomas J. Richardson, Samuel S. Mao
Lawrence Berkeley National Laboratory (LBNL)
MS 70-108B, One Cyclotron Road
Berkeley, CA 94720
Phone: (510) 486-8619; Fax: (510) 486-8619
E-mail: tjrichardson@lbl.gov

DOE Technology Development Manager:
Monterey R. Gardiner
Phone: (202) 586-1758; Fax: (202) 586-9811
E-mail: Monterey.Gardiner@ee.doe.gov

DOE Project Officer: Katie Randolph
Phone: (303) 275-4901; Fax: (303) 275-4753
E-mail: Katie.Randolph@go.doe.gov

Contract Number: DE-FG36-05GO15002

Start Date: December 1, 2004
Projected End Date: 2009

Objectives

- Bring together an eclectic group of scientists with experience in materials discovery and theoretical prediction of properties to work on developing new types of hydrogen storage materials.

Particular emphasis is placed on exploring the possibilities of the following types of materials for meeting the 2010 DOE hydrogen storage system targets, especially specific energy, energy density, durability, and uptake and discharge kinetics:

- nanoporous polymers
- nanoporous coordination solids
- destabilized high-density hydrides
- nanostructured boron nitride
- magnesium and light alloy nanocrystals

Note that only the research on nanoporous polymers, nanoporous coordination solids, and destabilized high-density hydrides is funded through this

award, with the other subprojects being funded through Basic Energy Sciences.

Technical Barriers

This project addresses the following technical barriers from the On-Board Hydrogen Storage section of the Hydrogen, Fuel Cells and Infrastructure Technologies Program Multi-Year Research, Development and Demonstration Plan:

- (B) Weight and Volume
- (C) Efficiency
- (D) Durability
- (E) Refueling Time
- (M) Hydrogen Capacity and Reversibility
- (N) Lack of Understanding of Hydrogen Physisorption and Chemisorption

Technical Targets

The main focus will be on meeting the following specific targets and those in Table 1:

- By 2010, develop and verify on-board hydrogen storage materials achieving storage system targets of 2 kWh/kg (6 wt%), 1.5 kWh/L, fill time of 3 minutes for 5 kg of hydrogen, and \$4/kWh.

FY 2009 Accomplishments

- Synthesized and characterized the first beryllium-based metal-organic framework: $\text{Be}_{12}(\text{OH})_{12}(\text{BTB})_4$ with a Brunauer-Emmett-Teller (BET) surface area of 4,020 m^2/g .
- Performed high-pressure H_2 adsorption measurements on $\text{Be}_{12}(\text{OH})_{12}(\text{BTB})_4$, revealing good H_2 storage characteristics at 77 K, with maxima of 6.0 excess wt% at 20 bar and 57 g/L at 50 bar.
- Performed detailed characterization of $\text{Mg}_2(\text{DOBDC})$, a metal-organic framework featuring open Mg^{2+} coordination sites H_2 within air-free $\text{Zn}_4\text{O}(\text{BDC})_3$, revealing an initial isosteric heat of H_2 adsorption of ca. -12 kJ/mol and binding of D_2 at a distance of 2.5 Å from the metal center.
- Synthesized and characterized a series of metal-organic frameworks of the type $\text{M}_3(\text{BTC})_2$ ($\text{M} = \text{Cr}, \text{Mn}, \text{Co}, \text{Zn}, \text{Mo}$) featuring open metal coordination sites.

TABLE 1. On-Board Hydrogen Storage System Targets (**Data is based on material only, not system value)

Storage Parameter	Units	2010 System Target	Fiscal Year 2009 materials**
Specific Energy	kWh/kg (wt% H ₂)	2.0 (6 wt%)	7.1 excess wt% at 77 K and 40 bar for air-free Zn ₄ O(BDC) ₃ (SA 3,800 m ² /g)
Specific Energy	kWh/kg (wt% H ₂)	2.0 (6 wt%)	11.5 total wt% at 77 K and 170 bar for air-free Zn ₄ O(BDC) ₃ (SA 3,800 m ² /g)
Specific Energy	kWh/kg (wt% H ₂)	2.0 (6 wt%)	2.3 wt% at 298 K and 70 bar for air-free Zn ₄ O(BDC) ₃ (SA 3,800 m ² /g)
Energy Density	kWh/L (g H ₂ /L)	1.5 (45)	77 g H ₂ /L at 77 K and 170 bar for air-free Zn ₄ O(BDC) ₃ (SA 3,800 m ² /g)
Specific Energy	kWh/kg (wt% H ₂)	2.0 (6 wt%)	6.0 excess wt% at 77 K and 20 bar for Be ₁₂ (OH) ₁₂ (BTB) ₄ (SA 4,020 m ² /g)
Energy Density	kWh/L (g H ₂ /L)	1.5 (45)	57 g H ₂ /L at 77 K and 50 bar for Be ₁₂ (OH) ₁₂ (BTB) ₄ (SA 4,020 m ² /g)
Specific Energy	kWh/kg (wt% H ₂)	2.0 (6 wt%)	3.8 wt% at 77 K and 45 bar for hypercrosslinked polystyrene (SA 1,930 m ² /g)
Specific Energy	kWh/kg (wt% H ₂)	2.0 (6 wt%)	1.9 wt% at 77 K and 23 bar for hypercrosslinked polyaniline (SA 630 m ² /g)

SA - surface area

- Generated N-linked microporous polymers exhibiting extremely small pore sizes, leading to an initial isosteric heat of adsorption of ca. -18 kJ/mol.
- Investigated new methods for synthesizing hypercrosslinked polypyrroles. With a BET surface area of 732 m²/g, the best sample exhibited reversible H₂ uptake of 1.6 wt% at 77 K and 40 bar.
- Utilized computational methods in examining changes in H₂ binding energies within the clusters [M₄Cl(tetrazolate)₈]¹⁻ (M = Mn, Cu, Zn).
- Investigated hydrogen storage in mixtures of MgH₂ and MgF₂. With 3 mol% MgF₂, the results showed desorption performance very similar to the results previously obtained with 10 mol% MgF₂.
- Performed elemental mapping by electron energy loss spectroscopy (EELS) to show that in the 3 mol% samples, the fluoride is well dispersed over the particle surface.



Introduction

Known hydrogen storage materials exhibiting promise include nanostructured carbon-based solids,

chemical hydrides, and metal hydrides. Although worthy of significant further investigation, it is by no means clear that any of these systems will be able to meet the DOE performance targets for 2010. We are therefore undertaking a broad-based and coordinated effort to search for new classes of hydrogen storage materials.

Approach

The combined team of UCB and LBNL have formed a collaborative, interdisciplinary group to research promising nanostructured materials for hydrogen storage. A total of eight themes or subprojects are currently underway; the following four are funded through this award:

- Synthesis and characterization of nanoporous coordination solids (Long).
- Synthesis and characterization of nanoporous polymers (Fréchet).
- First-principles determination of H₂ binding energies with predictive applications in design of new nanoporous hydrogen storage materials (Head-Gordon).
- Synthesis and characterization of destabilized high-density hydrides (Richardson).

Our approach will be to explore numerous possibilities for new materials, and narrow our focus as the research progresses. The synergy of many scientists in one location working toward a common goal is expected to accelerate our progress and lead to new ideas via cross-fertilization.

Results

Microporous Metal-Organic Frameworks – Until recently, our reports have mainly focused on the synthesis of metal-organic frameworks comprising transition metal atoms or clusters as building blocks. We have recently initiated a survey of group 2 and 13 main group elements, namely beryllium, magnesium, calcium and aluminum, as potential candidates for building light-weight materials. The interest in these compounds is strongly coupled with the expectation that their high charge-to-size ratio will provide more polarizing metal centers to serve as high-enthalpy adsorption sites for hydrogen molecules.

Beryllium perhaps represents the ultimate lightweight main group element for building metal-organic frameworks, and we are currently unaware of any examples of extended porous structures incorporating this element. In our previous report we described in detail the synthesis, characterization and preliminary hydrogen storage properties of a novel beryllium-based metal-organic framework,

$\text{Be}_{12}(\text{OH})_{12}(\text{BTB})_4$ (**1**, $\text{BTB}^{3-} = 1,3,5$ -benzenetribenzoate), shown in Figure 1.

The physical properties of activated single-crystalline samples of **1** have been recently studied. The BET surface area is $4,020 \text{ m}^2/\text{g}$ (Langmuir $4,400 \text{ m}^2/\text{g}$), which is the highest recorded so far for a main group metal-organic framework. This far exceeds the value of approximately $1,000 \text{ m}^2/\text{g}$ we reported for the same compound in our previous report, highlighting the importance of optimizing the synthetic and activation procedures. The current result broadly agrees with the accessible surface area computed from the crystal structure of approximately $3,600 \text{ m}^2/\text{g}$. Samples of **1** allowed to stand in air following activation showed no decomposition over 12 h, which is a contrast to other high-surface area materials such as $\text{Zn}_4\text{O}(1,4$ -

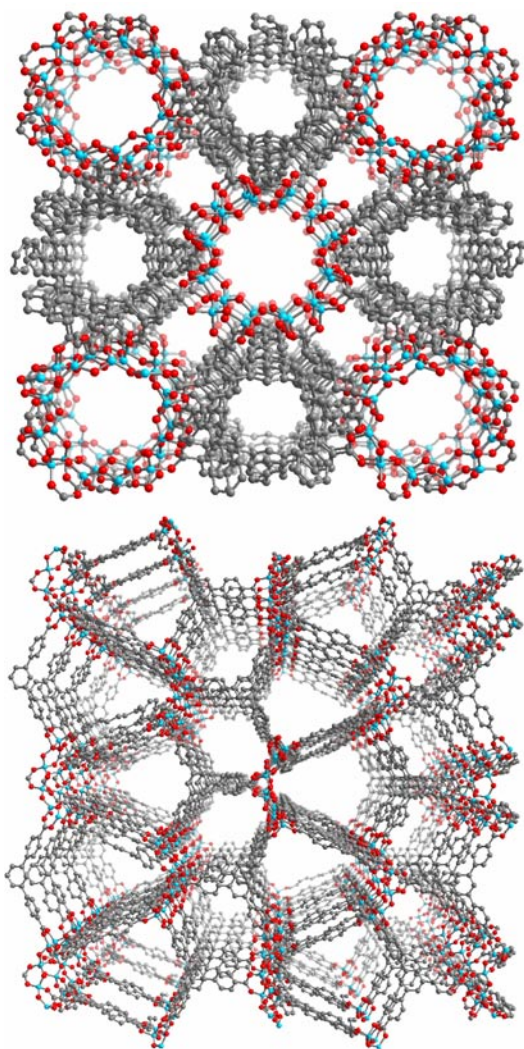


FIGURE 1. A portion of the single-crystal structure of $\text{Be}_{12}(\text{OH})_{12}(1,3,5\text{-benzenetribenzoate})_4$, **1**, projected along the crystallographic *c*-axis (left) and *b*-axis (right). Blue, gray, and red spheres represent Be, C, and O atoms, respectively. H atoms have been omitted for clarity.

benzenedicarboxylate) (MOF-5) which degrades rapidly upon exposure to the air.

The hydrogen storage properties of **1** have also been examined. As shown in Figure 2, the uptake recorded at 1 bar of hydrogen at 77 K is 1.6 wt% (1.3 wt% for MOF-5 under the same conditions), and the profiles are indicative of a low isosteric heat of adsorption. Indeed, a virial fitting of the experimental data yields an initial isosteric heat of adsorption of approximately 5.5 kJ/mol. While this result precludes hydrogen storage at room temperature, which requires an isosteric heat of adsorption of approximately 20 kJ/mol, it is promising for cryogenic storage applications. High-pressure hydrogen uptake measurements at 77 K have indicated that this is the case, with approximately 6.0 excess wt% adsorbed at 20 bar, and 8.0 total wt% adsorbed at 40 bar (see Figure 2). The volumetric storage capacity of 57 g/L is competitive with the most effective metal-organic frameworks in cryogenically storing hydrogen.

We have also begun a hydrogen uptake study on the recently reported magnesium-containing framework, $\text{Mg}_2(\text{DOBDC})$ ($\text{H}_4\text{DOBDC} = 2,5$ -dihydroxyterephthalic acid). This compound is of interest due to the presence of unsaturated coordination sites on the Mg^{2+} ions, which may act as strong binding sites for hydrogen. Initial experiments have indicated that the initial isosteric heat of adsorption for hydrogen in this compound is 11-12 kJ/mol, and the hydrogen uptake in the low-pressure region is high ($>2.5 \text{ wt}\%$ at 1 bar). Although this compound and a number of its isostructures has been the subject of a hydrogen adsorption study, both the binding strength and hydrogen uptake is higher in our hands, possibly highlighting the importance of using the correct synthetic and handling procedures when performing manipulations on this compound. We are currently performing further studies on the hydrogen binding sites

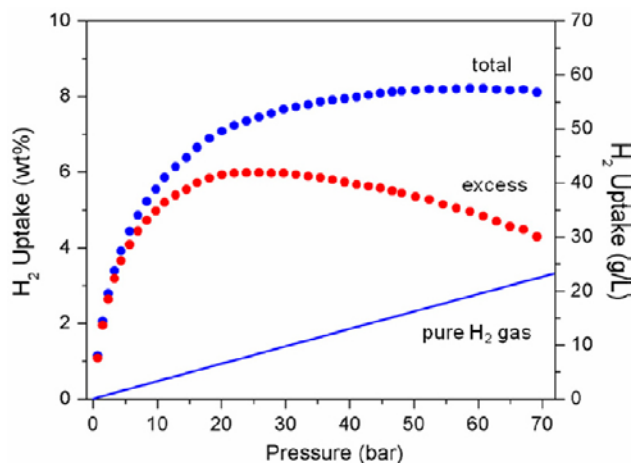


FIGURE 2. High-pressure hydrogen uptake data for $\text{Be}_{12}(\text{OH})_{12}(1,3,5\text{-benzenetribenzoate})_4$, **1**.

in this compound by infrared and Raman spectroscopy, and neutron diffraction in collaboration with the National Institute of Standards and Technology (NIST). While these experiments are ongoing, initial results from the neutron diffraction experiments have allowed us to locate the hydrogen atoms within the structure, with the centroid of the H₂ molecule located approximately 2.5 Å from the Mg²⁺ site. It is hoped that the results of these studies will allow us to better understand the nature and strength of the interaction between hydrogen and the unsaturated metal site, and furthermore, the knowledge gained may serve as a basis for designing new target materials for use as hydrogen storage materials.

The adsorption enthalpy for hydrogen binding to activated metal-organic frameworks is one of the limiting factors for accessing appreciable storage of this gas at ambient temperature. To ascertain which metal ion affords the maximal hydrogen binding enthalpy, we have continued to focus on synthesizing and characterizing the gas-uptake properties of a series of isostructural frameworks in which only the metal is varied. Frameworks containing dimetallic clusters bridged by four carboxylate groups are attractive targets as this building unit is a common motif in coordination chemistry.

The synthesis of Zn₃(BTC)₂, Cu₃(BTC)₂, Cr₃(BTC)₂ and Mo₃(BTC)₂ were reported previously, either in the literature or communicated by our lab. The chromium(II) framework shows a moderate hydrogen binding enthalpy at -6.8 kJ/mol with a gravimetric storage capacity of 2.1 wt% at 77 K. Powder neutron diffraction experiments carried out at NIST on activated Cr₃(BTC)₂ indicate that hydrogen binds tightly to a hydrophobic pocket within the framework as well as the exposed metal center. Rietveld analysis revealed a short distance between the metal ions (2.05 Å) that lengthens upon hydrogen binding (2.17 Å). Together with a moderate adsorption enthalpy (-6.8 kJ/mol), these data suggest that there is bonding between the chromium(II) ions which, expectedly, weakens hydrogen binding at the vacant axial coordination site. Hydrogen uptake by Zn₃(BTC)₂ might be predicted to be greater than the chromium(II) analogue because no metal-metal bond exists in the former. However, attempts to activate the zinc(II) framework by evacuating guest solvent at elevated temperatures resulted in a loss in crystallinity and porosity. We are currently exploring alternate methods for activating this material, such as treatment with supercritical carbon dioxide.

Recently, we have synthesized Mn₃(BTC)₂ and Co₃(BTC)₂, which was confirmed by powder and single-crystal X-ray diffraction experiments that these compounds are isostructural with other M₃(BTC)₂ frameworks. Infrared spectra of the solid strongly suggest that the open-coordination site at the metal ion is occupied by *N,N*-dimethylformamide (DMF).

Typically, these DMF molecules are exchanged for lower boiling alcohol solvents, which allows for milder desolvation temperatures. These frameworks however lose crystallinity as observed by changes in the powder X-ray diffraction patterns upon exposure to air or soaking in protic solvents. At present, we are investigating conditions to increase the current synthetic scale and activate these compounds for hydrogen-uptake measurements.

Microporous Polymers – We continued our studies focused on the preparation of hypercrosslinked polymers with large surface areas. The concept of the hypercrosslinking requires that the polymer to be crosslinked must be dissolved or swollen with a solvent and then crosslinked at a reaction rate that is faster than the rate of desolvation of the polymer chains. If this condition is not met, the resulting polymer is not porous.

In our specific study, we targeted networks consisting of aromatic rings held in a porous framework by the smallest possible linking groups. The reasons for this approach were twofold. First, we have shown previously that nanoporous polymers prepared via hypercrosslinking using smaller, more rigid crosslinks exhibit higher surface areas than those synthesized with longer less rigid crosslinks. Second, smaller crosslinks add less non-adsorbing mass to the final porous material. We also wanted to avoid the presence of electron withdrawing substituents on the aromatic rings since we have already demonstrated that addition of electron withdrawing groups to aromatic rings decreases their ability to physisorb hydrogen.

The simplest approach to forming networks consisting of aromatic rings starts with precursors containing reactive groups directly attached to the aromatic ring such as aryl halides and amines, which can be coupled using a variety of synthetic routes. For example, the Ullman reaction catalyzed with soluble or insoluble copper salts and the Buchwald reaction which relies on soluble palladium catalysts are used often to perform such couplings. Both of these syntheses were applied to the crosslinking of aryl amines with polyhalogenobenzenes to form amine-linked networks of aromatic rings. Thus crosslinking with tribromobenzene affords networks of di- and tri-functionalized aromatic rings connected by amines whereas crosslinking with diiodobenzene or dibromobenzene leads to a network of difunctionalized aromatic rings. While the substituted benzenes can be considered crosslinkers from the synthetic point of view, the final product is in fact a network of aromatic rings connected through nitrogen atoms. The resulting porous polymer networks consist of aromatic rings linked through a trivalent nitrogen atom. The Buchwald reaction appears to be more effective than the Ullman synthesis for the production of such materials. The use of solvents with higher Hildebrand solubility coefficients during synthesis affords polymers

with higher surface areas. The nanoporous polymers possess unusually high initial enthalpies of adsorption of hydrogen reaching values of up to -18 kJ/mol which appear suitable for the adsorption at temperatures higher than 77 K. Hypercrosslinked polymer networks we synthesized contained 37-92% of pores small enough for hydrogen adsorption but too small to allow penetration of nitrogen thus enabling size-selective gas adsorption.

We have also synthesized a series of nanoporous polypyrroles using a variety of different crosslinking units to control pore size. For example, polypyrrole base was crosslinked with diiodomethane. With remarkably high BET and Langmuir surface areas of 732 and 543 m^2/g , the resulting polymer reversibly adsorbs 1.6 wt% hydrogen at 77 K and 0.4 MPa. In order to explore the effect of the number of bonds linking the crosslinker with polypyrrole on the porous properties of our materials, we also used iodoform to crosslink polypyrrole base. This reaction produced materials which reversibly adsorb 1.3 wt% H_2 at 77 K and 0.4 MPa and exhibits BET and Langmuir surface areas of 401 and 436 m^2/g , respectively. The amount of residual iodine in the final product is undetectable by elemental analysis.

Polypyrrole was also hypercrosslinked with boron. This novel synthesis results in a mixture of polypyrrole rings crosslinked with boron atoms. Although crosslinking was incomplete, this polymer exhibits BET and Langmuir surface areas of 19 and 233 m^2/g . Although the largest reported, the surface area of our polymers was relatively small and the polymer adsorbs only 0.6 wt% hydrogen at 77 K and 0.1 MPa. Therefore, we continued the study in order to optimize the choice of both solvent and base. Unfortunately, good solvents of polypyrrole such as dimethylformamide, N-methyl pyrrolidinone, and dimethyl sulfoxide could not be used as they react violently with boron triiodide, while solvents that are typically used with borohalides like diethyl ether and tetrahydrofuran, are very poor solvents for polypyrrole. Finally, toluene, which is a mediocre solvent for polypyrrole but only forms weak complexes with boron triiodide was selected. The choice of bases also requires some compromises as hindered organic bases such as triethylamine and diisopropylethylamine react rapidly with boron triiodide while most inorganic bases have little solubility in toluene. Thus, a very fine powder of cesium carbonate was chosen as the optimal base for this reaction.

However, we prepared again polymer with nanoporosity enabling exclusion of gas molecules larger than hydrogen based on their size. For example, the adsorption of hydrogen was about 5 times higher than that found for nitrogen. This result is important since it may enable selective adsorption of pure hydrogen from its mixtures with other gases that are typically present in the industrially produced hydrogen.

We also tested additional metals to achieve hypercrosslinking and form a metal-organic network. For example, iron trichloride crosslinks polypyrrole in the presence of dimethylsulfoxide and sodium t-butoxide. This reaction so far affords a polymer with a relatively low BET surface area of 116 m^2/g .

Computational Studies of H_2 Binding – We have been engaged in modeling the hydrogen-binding center in the compounds synthesized in the Long group, beginning with $\text{Mn}_3[(\text{Mn}_4\text{Cl})_3(\text{BTT})_8(\text{CH}_3\text{OH})_{10}]_2$ ($\text{H}_3\text{BTT} = 1,3,5$ -tris(tetrazol-5-yl)benzene). From there, we moved to consider both substitutional replacements of the Mn^{2+} counterion, as performed experimentally, and substitutional replacements of the central (Mn_4Cl) unit with (Zn_4Cl) and (Cu_4Cl) units. A single site, with tetrazolate anions replacing the BTT ligands is treated. In the experimental compounds, these binding centers are overall negatively charged, which is compensated by dications that populate half the sites. We have worked through and substantially resolved most of the computational protocol issues associated with appropriate selection of density functional, integration grid, and treatment of the metal center. A large series of calculations is underway treating sites of both charges and the various substitutional replacements. We anticipate being able to complete both detailed comparison against existing experimental data, as well as provide some indication of the scope for improved binding coming from alternative metals.

Destabilized Metal Hydrides – We reported previously that addition of 10 mol% magnesium fluoride to magnesium hydride enhanced the sorption/desorption kinetics and greatly improved the utilization of MgH_2 . This has now been extended to mixtures containing 3 mol% and 1 mol% MgF_2 . The desorption behavior at 673 K for the three mixtures and for commercial MgH_2 are shown in Figure 3. The results are near theoretical

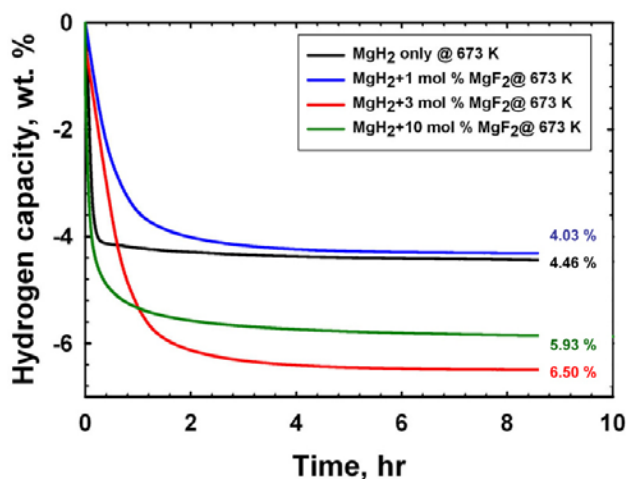


FIGURE 3. Effects of addition of MgF_2 on MgH_2 hydrogen desorption.

for 10% and 3% MgF_2 , the higher percentage for the latter due to the increased weight percentage of active MgH_2 . The improved performance persisted at a more constant level for the 3% case. While 1% addition had a positive effect on the utilization, the added weight reduced its capacity relative to pure MgH_2 , and the kinetics were worse. We believe that this is due to incomplete dispersion of the MgF_2 on the MgH_2 surfaces.

Elemental mapping by electron energy loss spectroscopy (EELS) of a ball-milled 3% MgF_2 sample showed that the fluoride was well dispersed over the particle surface (see Figure 4). As no evidence has been found by X-ray diffraction for dissolution of fluoride in the hydride or metal phases, we postulate that the mechanism by which fluoride acts is to coat the surfaces and prevent coarsening and sintering of Mg during desorption. This then enhances hydrogen uptake by maintaining the metal as small particles. High-resolution transmission electron microscope images of hydrogen-desorbed fluoride-treated Mg particles showed sharp faceting with a small grain size. On the other hand, without fluoride, sintering and coarsening reduced the surface area and contribute to isolation and poor utilization of Mg.

Fluoride addition appears to be a simple and inexpensive route to improving the hydrogen storage properties of magnesium hydride. Unlike metal catalysts, its effects persist over many cycles due to its mode of action on the particle morphology rather than on hydrogen splitting and recombination.

Conclusions and Future Directions

Synthetic approaches have now been developed for incorporating high concentrations of metal carbonyl units within nanoporous coordination solids and polymers. Methods for displacing CO are now under investigation, and will be followed by H_2 storage measurements for these unique materials. In addition, electronic structure calculations are underway to assess the best combinations of metal center and ligand substituents to adjust the H_2 binding energy.

FY 2009 Publications

1. "Hydrogen Storage in Microporous Metal-Organic Frameworks with Exposed Metal Sites" Dinca, M.; Long, J.R. *Angew. Chem., Int Ed.* 2008, 47, 6766-6779.
2. "Preparation of Size-Selective Nanoporous Polymer Networks of Aromatic Rings: Potential Adsorbents for Hydrogen Storage" Germain, J.; Fréchet, J.M.J.; Svec, F. *Chem. Mater.* 2008, 20, 7069-7076.
3. "Nanoporous, Hypercrosslinked Polypyrroles: Effect of Crosslinking Moiety on Pore Size and Selective Gas Adsorption" Germain, J.; Fréchet, J.M.J.; Svec, F. *Chem. Commun.* 2009, 1526-1528.

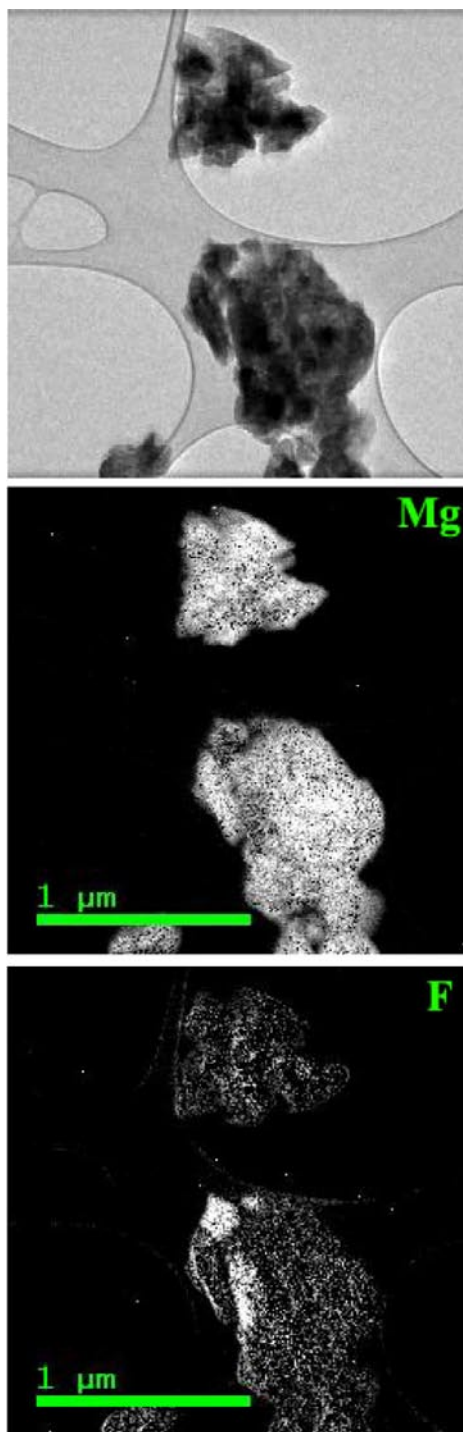


FIGURE 4. EELS maps showing the uniform, but granular distribution of MgF_2 particles on the surfaces of dehydrated Mg grains.

4. "Hydrogen Storage in Metal-Organic Frameworks" Murray, L.J.; Dinca, M.; Long, J.R. *Chem. Soc. Rev.* 2009, 38, 1294-1314.
5. "Nanoporous Polymers for Hydrogen Storage" Germain, J.; Fréchet, J.M.J.; Svec, F. *Small* 2009, 1098-1111.

FY 2009 Presentations

1-16. “Hydrogen Storage in Metal-Organic Frameworks”
Long, J. R.: Leiden University (July 14, 2008); Solid State Chemistry Gordon Research Conference, New London, NH (July 29, 2008); Boston University (September 29, 2008); Ewha Womans University (November 7, 2008); Seoul National University (November 10, 2008); Korea University (November 11, 2008); Osaka University Forum on Bio-Environmental Chemistry, San Francisco, CA (December 10, 2008); University of Chicago (February 23, 2009); American Physical Society Meeting, Pittsburgh, PA (March 18, 2009); University of Pittsburgh (March 19, 2009); The 237th Meeting of the American Chemical Society, Salt Lake City, UT (March 23, 2009); ADVANCE Distinguished Lecture, Dept. of Chemical Engineering, Kansas State University (April 7, 2009); University of North Carolina, Chapel Hill (April 14, 2009); Wake Forest University (April 15, 2009); UCLA (April 22, 2009); EC Workshop on Hydrogen Storage, Crete, Greece (June 12, 2009).